

How about that Bayes: Bayesian techniques and the simple pendulum

Matthew Heffernan^{1,*}

¹*Department of Physics, McGill University, 3600 University Street, Montreal, QC, H3A 2T8, Canada*

Physics increasingly relies on Bayesian techniques for rigorous data analysis and model-to-data comparison. This paper describes how these methods can be implemented to answer questions of relevance to teaching laboratories. It demonstrates the Bayesian approach to statistical modeling and model selection in a rigorous step-by-step workflow. The example of the simple pendulum allows for a demonstration with the precision commonly seen in student measurements in the introductory laboratory. This can be used to provide realistic quantitative guidance for model preference between the small angle approximation and more complicated formula. This extends the current simple pendulum literature's focus beyond comparing individual idealized assessments of different approximations and places such discussions on a data-driven foundation while providing actionable guidance for teaching laboratory design.

I. INTRODUCTION

Introductory physics courses commonly teach that the period of a simple pendulum displaced by a small angle may be found by applying the approximation $\sin \theta \approx \theta$, which applies when θ is small. However, the period of a pendulum also depends on the initial angular displacement. Attempts to increase accuracy in approximations of the pendulum period have so far focused on more closely approximating the full non-analytic integral expression for the period so students in undergraduate laboratories can investigate the dependence of the period on initial angular displacement [1]. Recently, model comparison and complexity has been applied to the pendulum problem or the teaching laboratory [2].

Guidance for the use of the small angle approximation in simple pendula has not previously been rigorously quantified using realistic uncertainties measured in teaching laboratories. Often, the only suggestion is that after $\sim 15^\circ$, the difference between $\sin \theta$ and θ in radians exceeds 1% and the small angle approximation should no longer be used [3]. This does not take into account the variety of measurement uncertainties detailed in introductory physics laboratory materials or if more elaborate formulae are demanded by the data. This study demonstrates that students with both an exact and approximate analytical formula for the period of a pendulum could successfully establish a quantitative preference between the two at moderate displacements using Bayesian tools. This can also be extended to the case of choosing between various more

complex approximations. This study remedies a gap in the literature by quantitatively motivating more complex formula in teaching laboratories via realistic measurements and will provide guidance to instructors and their students in restricting the initial angular displacement or employing a more complex formula (c.f. [4] for a recent review).

This paper will demonstrate how to establish these quantitative criteria by introducing and demonstrating the techniques of Bayesian data analysis. Using Bayesian model selection, a quantitative preference between the small angle approximation and a numerical calculation of the exact integral equation is determined. First, an introduction to Bayesian statistics is provided. The exact expression for the period of a simple pendulum is derived as well as the small angle approximation to establish the Physics background. It is then established via prior predictive distributions that it is possible to differentiate the two formula in the presence of realistic measurement uncertainties. This is followed by Bayesian inference to fit the models to data; first to pseudodata generated by each individual model to determine that the statistical power of the analysis is sufficient and then to measurements of the period of a simple pendulum taken with apparatus available in the undergraduate teaching laboratory. The posterior distribution is then analyzed and posterior predictive checks are made and are consistent with expectations. Finally, it is determined at what initial angular displacement weak, moderate, and strong preference for the exact calculation are found given realistic, but precise, measurements in the absence of nonconservative forces. This preference can be used to inform recommendations of

* heffernan@physics.mcgill.ca

maximum initial angular displacement in laboratory materials and textbooks and as a general introduction to Bayesian techniques for implementation in the undergraduate physics curriculum.

II. BAYESIAN STATISTICS

Bayesian data analysis is an increasingly commonly used tool in physics research, e.g. gravitational-wave astronomy [5] and recently in ultra-relativistic heavy ion collisions [6], among many others [7]. The techniques and process are similarly ripe for application to pedagogical questions.

In Bayesian statistics, probability is interpreted as the degree of belief in a proposition given the available data and prior knowledge. Put another way, Bayesian statistics quantifies the plausibility or betting odds of a proposition being true. The Bayesian approach is well-suited to applications with limited data where other common-sense knowledge may exist – a description that fits the introductory laboratory well.

The central theorem of Bayesian statistics is Bayes' theorem,

$$p(H|d, I) = \frac{p(d|H, I) p(H|I)}{p(d|I)}. \quad (1)$$

Throughout this work, $p(\cdot)$ denotes probability and the vertical bar in $p(\cdot|\cdot)$ denotes conditionality, i.e. $p(A|B, C)$ should be read as the probability of A given B and C . A colloquial description of Bayes' theorem is that it formalizes the idealized process of learning: a prior belief is compared with data. Based on how well it matches the observation, the prior belief is determined to be relatively more or less likely. This updated understanding forms the posterior belief. More formally, $p(H|I)$ is called the “prior” and represents the belief in the hypothesis H prior to comparison with measurements. $p(d|H, I)$ is the “likelihood” and is the likelihood for the data d to be true given the hypothesis H . $p(d|I)$ is the “Bayes evidence” and is typically treated as a normalization constant such that $\int p(H|d, I)dH = 1$. It quantifies how likely one believes the data to be given other information I , which can include a given model in which a particular choice of parameters forms a hypothesis H . I also denotes any other additional information such as reasonable expectations that are

not informed by d , such as expectations from first-principles theory. $p(H|d, I)$ is called the “posterior” and quantifies the belief in any hypothesis H posterior to comparison with measurement data d .

Bayes' theorem may be used to solve problems by inversion, asking “how likely is the data given a set of model parameters” (the likelihood) in order to answer the primary question of interest, “how likely is the set of model parameters given the data” (the posterior). Consequently, a hypothesis for which the observed data is unlikely is itself an unlikely hypothesis. These concepts will be demonstrated using the familiar case of the simple pendulum.

In practice, the hypothesis H often represents a particular choice or distribution of parameter(s). Special cases, called conjugate priors, exist where the posterior can be found in closed form. In most applications, these special cases are not ideal for the problem at hand. When this is the case, Bayes' Theorem is numerically evaluated using computational tools such as Markov Chain Monte Carlo, from which the posterior may be constructed. This yields an estimate of the parameters of the model as well as any covariance structure, in turn allowing for the precise quantification of the degree of belief. An introduction to Bayesian inference, including contrasts with Frequentist statistics, can be found in [8–10]. A guide to rigorous Bayesian modeling may be found in [10–12].

In this study, Bayes' Theorem and related techniques will be used to determine when, given realistic data, it is possible to detect weak, moderate, and strong preference for the exact expression for the period of a pendulum relative to the expression for the period of a pendulum in the small angle approximation. To do so, realistically-generated pseudodata and principled prior expectations will be used in order to evaluate Bayes' Theorem (Eq. 1) in a rigorous modeling workflow. This study employs the use of the Gaussian likelihood function, usually represented in its logarithmic form, which assumes that uncertainties are normally distributed around a central value.

$$\ln p(d|H, I) = -\frac{1}{2} \sum_{i=1}^N \left[\ln(2\pi\sigma^2) + \frac{(d_i - Y_{\text{Model}})^2}{\sigma^2} \right], \quad (2)$$

where Y_{Model} is the model calculation of the period and $\sigma^2 = \sigma_{\text{data}}^2 + \sigma_{\text{model}}^2$. In this study, only one parameter – the gravitational acceleration g – will be varied and a particular value of g constitutes a

hypothesis H given the choice of model or other assumptions I . Generalizing to higher dimensions is beyond the scope of this work, but is well documented in standard introductory textbooks [9, 10].

III. THE PERIOD OF A SIMPLE PENDULUM

For completeness, the small angle approximation and the exact expression for the formula of a simple pendulum are derived. An ideal simple pendulum has a bob of mass m suspended from a frictionless attachment point by a massless rod of length L and moves in a single angular dimension θ . In the absence of nonconservative forces such as friction and drag, the equation of motion is

$$\ddot{\theta} = -\frac{g \sin(\theta)}{L} \quad (3)$$

where g is the gravitational acceleration. In this study, a fixed value $L = 0.807 \pm 0.0005\text{m}$ was measured on a standard laboratory apparatus available for use in introductory physics laboratory courses on a meter-stick with millimeter gradations. In line with common advice given in introductory laboratories, the quoted uncertainty corresponds to half of the smallest increment of the measuring device. The uncertainty on initial angular displacement corresponds to the use of digital protractor with 0.01 degree degradations; all angular model inputs thus have uncertainty $\pm 0.005^\circ$. For small displacements, $\sin \theta \approx \theta$ and Eq. 3 can be identified as a simple harmonic oscillator. The period of a simple harmonic oscillator is $T = 2\pi\sqrt{\frac{m}{k}}$ and it is trivial to identify $k = \frac{mg}{L}$. Consequently, in this regime,

$$T_0 = 2\pi\sqrt{\frac{L}{g}} \quad (4)$$

and the uncertainty on the angular measurement does not enter into the model calculation. An exact expression for the period of a simple pendulum is readily derived using the conservation of energy. The expression is simplified by assuming the pendulum to be initially stationary and at its initial angular displacement θ_0 . The zero of potential energy is chosen to be when $\theta(t) = 0$. The energy conservation equation is $mgL(1 - \cos \theta_0) = \frac{1}{2}mL^2\dot{\theta}^2 + mgL(1 - \cos \theta)$. It is then straightforward to solve for $\dot{\theta}$ and integrate θ from 0 to θ_0 , corresponding to one-quarter of the

period. This yields $T = 2\sqrt{2}\sqrt{\frac{L}{g}} \int_0^{\theta_0} \frac{1}{\sqrt{\cos \theta - \cos \theta_0}} d\theta$. This integral is improper when $\theta = \theta_0$, but a simple substitution $\cos \theta = 1 - 2 \sin^2(\theta/2)$ may be combined with a change of variables $\sin \phi = \frac{\sin(\theta/2)}{\sin(\theta_0/2)}$ to yield

$$T = 4\sqrt{\frac{L}{g}} \int_0^{\pi/2} \frac{1}{\sqrt{1 - \sin^2(\theta_0/2) \sin^2(\phi)}} d\phi \quad (5)$$

and may be evaluated numerically using tools such as SciPy [1, 13, 14]. Uncertainty on the initial angular displacement θ_0 is propagated with the assumption that this uncertainty is normally distributed and uncorrelated to the uncertainty in g . The small angle approximation (Eq. 4) and the exact expression (Eq. 5) are the models considered in this work.

A. Generating realistic measurements

In order to determine when the small angle approximation becomes insufficient using realistic measurements, realistic choices must be made. Using real measurements in order to determine model preference thresholds demands a sufficiently large number of measurements as to be impractical, so some of the data in this study is generated using Eq. 5 and assigning realistic uncertainties. Generated data used in model validation is termed “pseudodata”, real measurements are performed for the final inference, and generated data is used to calculate model preference thresholds. Pseudodata is generated for model validation by making a set of simple choices informed by experience in undergraduate teaching laboratories. In these laboratories, standard advice about the uncertainty is that the uncertainty of a measurement is equal to half of the smallest increment of the measurement device. A common measuring device in teaching laboratories includes meter sticks with millimetre gradations, corresponding to an uncertainty of $\pm 0.0005\text{ m}$. In teaching laboratories, more precise timing mechanisms such as photodiodes may also be available and the use of smartphone accelerometers in teaching laboratories has become more common [15]. The time step in these measurements is significantly more precise than the precision of a stopwatch and is not impacted by human reaction times. Common measurements with smartphone accelerometers in recent courses at McGill University had uncertainty of approximately $\pm 0.02\text{ s}$ [15] while timing uncertainties with the photodiode timer used in measurement are smaller still

at approximately ± 0.005 s. Finally, for timing uncertainties corresponding to the use of a stopwatch in model selection is taken to be $\sqrt{2}$ (0.250) s, corresponding to a reaction time of 0.250 s [16] to start and stop the timer added in quadrature. Advice given to students is to time up to 10 periods of a pendulum in order to reduce the relative error on the measurement, a process replicated in this work. This study assumes that measurements are normally distributed with standard deviation corresponding to the uncertainty.

Different values of the “true” gravitational acceleration and timing precision may be specified when generating pseudodata; it is then possible to specify the initial angular displacement and produce pseudodata that reflects the precision of data in introductory teaching laboratories. It is then demonstrated that the exact formula (Eq. 5) describes real data well, strongly supporting the use of the exact formula to generate data when taking measurements is impractical. It is possible to compare model predictions from the two methods of calculating the period of a simple pendulum to this realistically-generated data and establish ideal thresholds. A simple calculation is sufficient to show that the models become increasingly differentiable as θ_0 increases, but this work will examine when this differentiation translates into quantitative model preference. Generated data is used for this study in order to calculate an idealized limit of model preference without systematic biases from unaccounted-for physics.

IV. INFERENCE IN A RIGOROUS WORKFLOW

Reliable and robust data analysis requires a rigorous workflow. Following such a step-by-step process acts as a safeguard that ensures the validity of the analysis as well as a rich understanding of the models. In both research and pedagogical settings, clearly-defined steps are able to guide analysis, allow for careful implementation and refinement, and ensure that the final results are reliable. An additional benefit of a rigorous workflow for teaching is that it allows for the analysis to be broken into digestible, concrete steps that may be implemented in teaching materials.

The workflow presented here progresses from explicitly defining prior knowledge all the way to verifying that the final inference reproduces expecta-

tions. Each step is described, motivated, and implemented in the models already defined before progressing to the next step. At the end of the workflow, when both models have been validated and calibrated to data, Bayesian model selection is introduced to establish rigorous criteria for when the data itself demands one model over the other.

A. Step 1: Defining the prior state of knowledge

The first step in Bayesian data analysis, once the models have been defined, is to clearly motivate the choice of prior. Ideally, the choice of prior reflects concrete understanding of the parameter and is sufficiently general as to constrain the problem without pre-determining or biasing the result [17]. For example, a prior that precludes the true result by construction can never recover the true result. The goal of the prior is to be constraining, but allow for the bulk of the constraint on belief to be determined by the systematic comparison of the model to the data via the likelihood.

As the initial angular displacement and period of a simple pendulum are easily measured and the length of the pendulum has been fixed, the only free model parameter in both the equations using the small angle approximation and the exact expression for the period of a pendulum is the gravitational acceleration g . It is reasonable to assert *a priori* that for the period to be rigorously defined, g cannot be zero. As gravity is an attractive force and the period is positive, g must be positive definite. It is also possible to ascribe some degree of physical intuition to the problem. Gravitational acceleration on the surface of a body scales with the mass of the body and gravitational acceleration on the Moon is approximately 1.625 m/s^2 [18] and the surface gravity of Jupiter is 24.79 m/s^2 [19]. Proceeding with confidence that the mass of the Earth is likely between that of the Moon and Jupiter, a weakly-informative prior can be constructed that allows for some probability of surprise. A common choice for a weakly-informative prior on positive definite quantities is the inverse gamma distribution. The inverse gamma distribution has support on the interval $(0, \infty)$, matching the criteria we set and is easily tuned so that only 1% of the probability falls below 1.625 m/s^2 and above 24.79 m/s^2 . No positive real value has been ruled out, although some values have been de-

termined to be unlikely. This prior expectation for g is shown explicitly in Fig. 1. Note that the location of the mode of the distribution is not particularly relevant – by constructing a weakly-informative prior, the goal is that the information contained in the data will far outweigh the information in the prior. Other choices of prior that has similar support are possible, but the inverse gamma distribution has the nice feature of smoothly approaching 0 on the bounds of its support. This matches physical intuition. For example, if the prior set was the uniform distribution $U(1.625, 24.79)$, this would likely not change the results of the inference, but it would require justifying that 24.8 m/s^2 was infinitely less likely than 24.79 m/s^2 while all the values in between are equally likely.

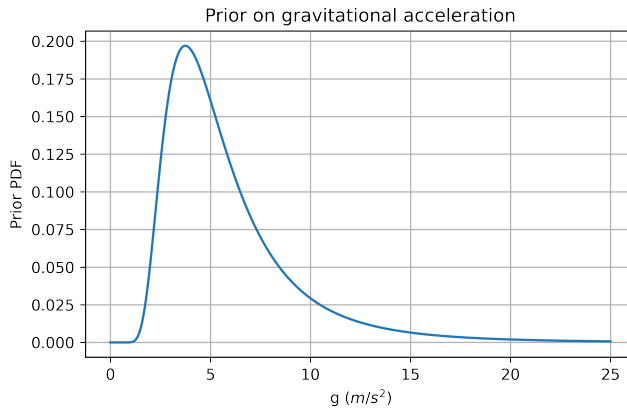


FIG. 1. (Color online) The proposed prior probability density function (PDF) of the gravitational acceleration g measured using a simple pendulum used in a teaching physics laboratory. This PDF is $p(H|I)$ in Eq. 1 where each value of g is a hypothesis H .

B. Step 2: Prior predictive checks

Prior predictive checking is an important step in gaining an understanding of model behavior [20]. In prior predictive checks, the computational model is evaluated with draws from the prior distribution. This is then used to assess the underlying model and determine the presence of non-trivial features or predictions that are at odds with expectations. In this simple case, a prior defined with support $[0, \infty)$ would suggest that a finite value for the period should be expected when the gravitational acceleration is 0. However, in this case, the period is

ill-defined and so the expectation is at odds with expectations. In more complex models, a non-trivial feature could be an interaction between two components of a multi-component model that yields unphysical results and should be excluded by a more carefully constructed prior. In this study, few of these features exist, but the step is still important in order to demonstrate a rigorous modeling procedure. Predictions for the period with g sampled according to the prior distribution are shown in Fig. 2. These are compatible with the prior knowledge defined in Sec. IV A. It is expected that measured periods of the pendulum are between approximately 1 and 5 seconds, while longer and shorter periods and corresponding values of g are still theoretically possible, but disfavored. The absolute difference between the two models is small relative to the impact of the gravitational acceleration, meaning that the result is highly sensitive to the parameter g .

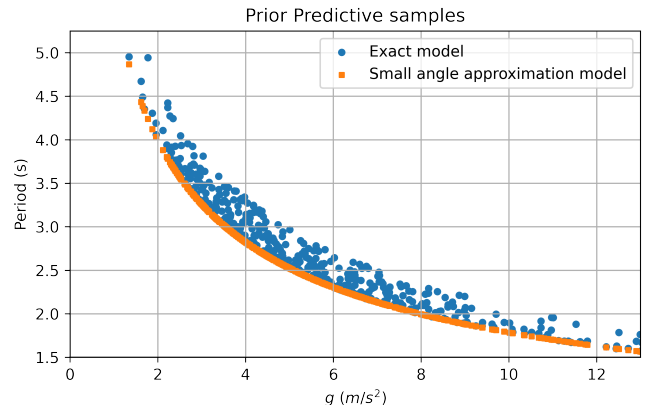


FIG. 2. (Color online) 100 predictions for the period with g sampled from the prior and initial angular displacement θ_0 sampled from a uniform distribution $U(0, \pi/4)$.

C. Step 3: Model validation

Model validation, also known as closure testing or empirical coverage, is a means of assessing whether the model has sufficient power to constrain the parameters given data. This is established by generating pseudodata with each model and using the same model that generated the data to see to what degree the parameters are constrained by the data and if the input value may be recovered when everything in the data is contained in the model. This is an important step as it represents the best-case scenario: the

model is known to contain all the physics in the data. While this may not be a large concern in this simple example, it is a critical feature in more intensive numerical applications with sophisticated observables, e.g. gravitational wave, cosmology, or heavy ion collision data analysis.

Validation pseudodata is generated with gravitational acceleration $g = 9.80665 \text{ m/s}^2$ corresponding to the NIST reference value [21] and a timing uncertainty corresponding to the use of a photodiode timer over 10 periods, comparable to the data used in the full inference. Initial displacements are chosen with arbitrary spacing, $\theta_0 = [0.05, 0.2, 0.35, 0.4, \pi/5]$ radians, and calculations of the corresponding periods are shown in Fig. 3. The models are then both

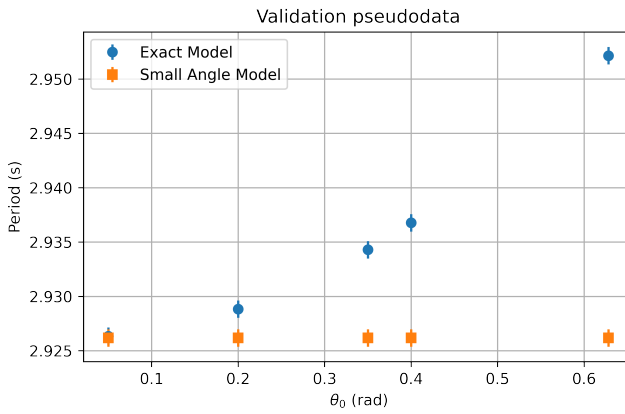


FIG. 3. (Color online) Pseudodata used for model validation.

calibrated to their respective validation pseudodata (Fig. 3) and the posterior distributions are shown in Fig. 4, where it can be clearly seen that both models are able to achieve closure when the data is perfectly consistent with the model. The small angle approximation model's posterior is slightly more peaked than that of the exact model because of the uncertainty from the angular measurement (the small angle approximation model has no angular dependence). For each parameter value considered, the likelihood (Eq. 2) is calculated and the value of the posterior can be computed. While this is simple in a small number of dimensions, this is impractical for high-dimensional applications and computing the posterior directly becomes computationally inefficient. To overcome this, the posterior is evaluated numerically using Markov Chain Monte Carlo (MCMC). MCMC algorithms are efficient sampling techniques in which “walkers” walk through the pa-

rameter space according to an algorithm. Each step taken by a walker is a sample and, when converged, the distribution of samples corresponds to a specified target distribution – in this case, the posterior specified in Eq. 1. The longer the walkers walk, the more samples are drawn and the distribution of those samples more closely resembles the distribution of interest. A chain of these samples can then be analyzed as draws from the posterior. This study uses a numerical implementation of MCMC that uses a parallel tempering algorithm, `ptemcee`, whose features allow for straightforward calculation of the Bayes evidence [22–24]. It is important to consider the MCMC be-

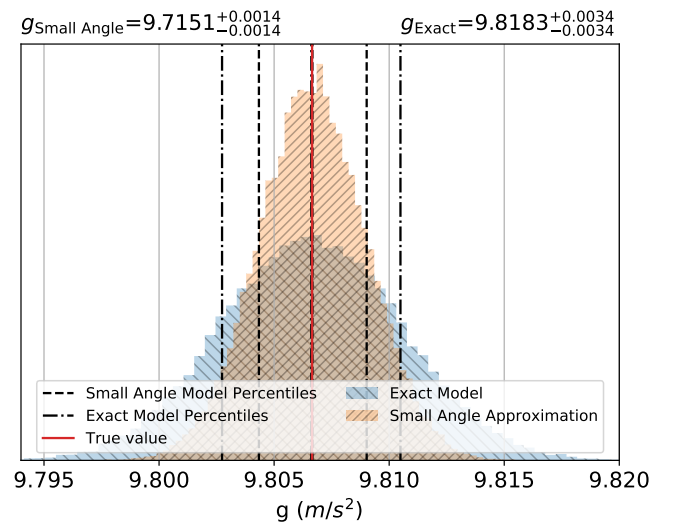


FIG. 4. (Color online) Posterior distributions for g in model validation using the exact formula for the period and the small angle approximation. The true value is shown in red and vertical dashed lines denote the 16th, 50th, and 84th percentile of the samples in increasing g . When the models contain the full information present in the data to which they are compared, both are able to recover the true value.

havior to ensure that the chains did in fact converge to their target distributions, i.e. that samples indeed approximate draws from the distribution of interest. This is most simply analyzed by considering autocorrelation, which quantifies how correlated samples are within a certain “lag”.¹ True independent samples of the posterior should be uncorrelated, while

¹ Autocorrelation is calculated by taking the inner product of the unshifted chain of samples with a chain shifted by the lag, normalized by the product of the magnitudes of the shifted and unshifted chains. As a result, the 0 lag autocorrelation is 1 by construction.

correlated samples suggest that the walkers are not taking random steps, but are walking in a particular direction and do not represent draws from the distribution of interest. The autocorrelation for the exact and small angle approximation MCMC chains are shown in Fig. 5, which show that after even a single step, the chain is uncorrelated and is sampling the target distribution successfully, uninfluenced by the previous step. The final check that must be performed

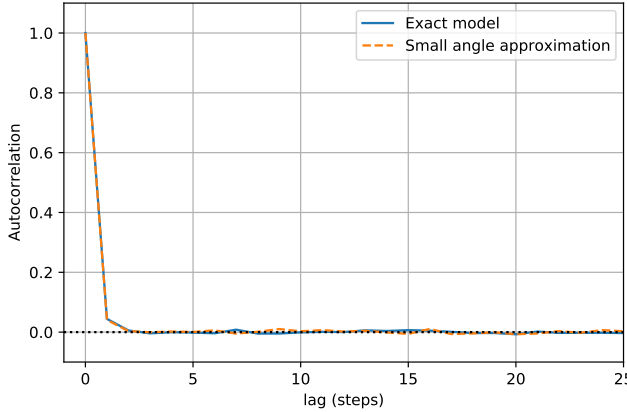


FIG. 5. (Color online) Autocorrelation of MCMC chains for model validation. The rapid drop and subsequent small-scale fluctuations around 0 are indicative of a decorrelated chain, meaning that the chain is sampling from the target distribution (the posterior).

before confidently progressing to the final inference is to consider the posterior predictive distribution, Fig. 6. Predictions can be made from the posterior distribution to form the posterior predictive distribution, which helps determine if the model truly behaves as anticipated by considering the distribution of results. If something has gone wrong in the inference or the MCMC, then the predictions made using the posterior distribution may not reproduce the data or may reveal underlying structure which is contrary to expectations but useful for improving the model. For example, the posterior predictive distributions may reproduce some of the data, but not other data, indicating that there is missing physics that is causing tension in the model. As expected from Fig. 4, where the models are calibrated to data generated by themselves, both models are able to successfully reproduce pseudodata. This is encouraging, as it is known by construction that there is no feature of the data that the respective models cannot account for. The distribution of model predictions are shown with violin plots, which

show distributional information analogously to box-and-whisker plots. In violin plots, the width of the blobs corresponds to the probability density of the data and is able to show more information than a box-and-whisker plot, allowing for more intuitive interpretation of the data.

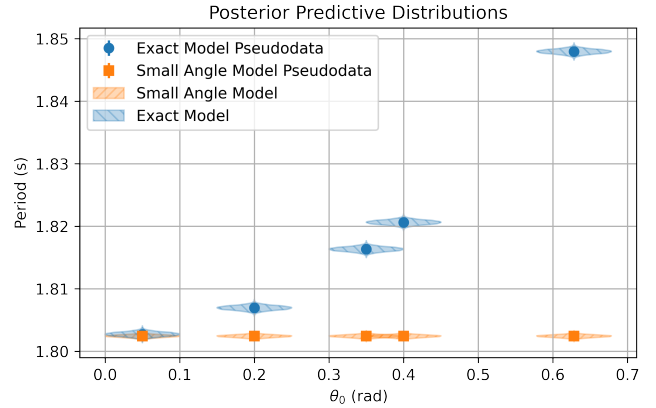


FIG. 6. (Color online) Violin plot of the prior and posterior predictive distributions for g from model validation. The posterior distributions are those shown in Fig. 4.

D. Step 4: Inference with data

After all the previous steps are completed, it is appropriate to systematically compare the models to real data. All the previous steps have indicated that the models should have discriminating power and should be capable of describing the data and have set expectations for the constraint.

Measurements were made with a pendulum of length $L = 0.807 \pm 0.0005$ m and a cylindrical bob of mass 10 ± 0.05 g with times recorded using a phototransistor connected to a Pasco 850 universal interface Model UI-5000 for data acquisition. Measurements of initial angular displacement θ_0 were made by a digital protractor and the bob was released from the same location with the guide of a stand to ensure uniformity of angle. 5 measurements of 10 periods were made at each angular displacement, consistent with the typical number of measurements performed by students in introductory teaching laboratories [15].

The posterior is evaluated numerically using MCMC, as performed and validated in the previous section. The posterior distribution for the gravitational acceleration g is shown in Fig. 7; the ex-

act model is able to infer the gravitational acceleration with a relatively precise 68% credible region – $9.818 \pm 0.003 \text{ m/s}^2$ – while the small angle approximation infers a result with higher precision – $9.715 \pm 0.001 \text{ m/s}^2$ – but sacrifices accuracy with a remarkable $\sim 0.1 \text{ m/s}^2$ bias from the standard value 9.80665 m/s^2 [21]. While the reference value is not within the 68% credible region of the exact model, the bias is greatly reduced and predictions with the posterior are investigated further in the next subsection and match the data well. The source of the difference in precision between the formula is readily interpretable: as the exact formula requires the propagation of uncertainty from the initial angular displacement, the posterior has a wider 68% credible interval than that of the small angle approximation which does not account for the angular displacement at all.

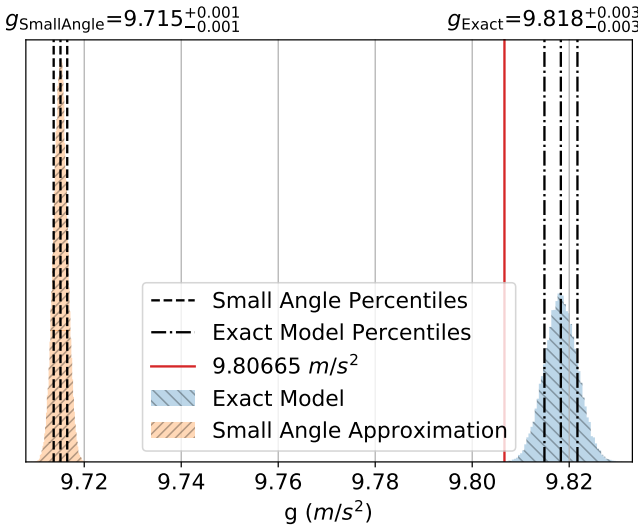


FIG. 7. (Color online) Independently normalized posterior distributions for g using the exact formula for the period and the small angle approximation. The standard value [21] is shown in red and vertical dashed lines denote the 16th, 50th, and 84th percentile of the samples in increasing g . This corresponds to the central value and the 68% credible interval.

E. Step 5: Posterior predictive checks

Now that the model has been calibrated to data, it is important to examine the posterior predictive distributions. This can also elucidate features of the predictions and provide insight as to why one model may fail to recover the expected result while

the other succeeds. These predictions are made by taking samples from the posterior and using them to make predictions for the period using the model in question. The distribution of these predictions forms the posterior predictive distribution (Fig. 8). The source of the bias in the small angle approximation model can be clearly seen in the posterior predictive distribution. The predictions from the exact model posterior are constrained around the measurements and are broadly consistent with the measured uncertainty, while the small angle model is biased by undershooting at large angular displacement and overshooting small displacements. As a result, the posterior predictive distributions make the incompleteness of the small angle approximation immediately apparent and interpretable. This clearly

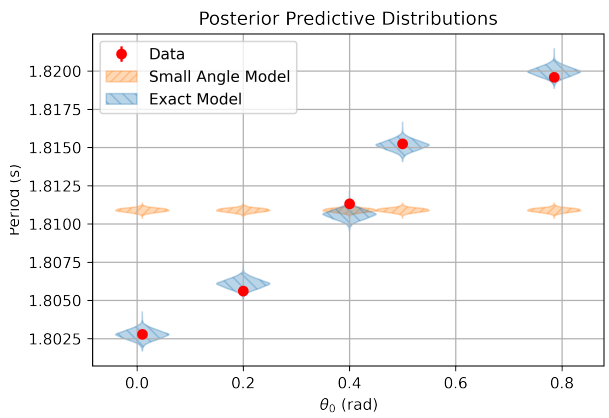


FIG. 8. (Color online) Violin plot of the posterior predictive distributions for g . The posterior distributions are those shown in Fig. 7.

establishes that it is possible to detect the bias in calculations of gravitational acceleration introduced by using the small angle approximation of the period of a pendulum while including large initial angular displacements and realistic measurement uncertainties. Through the use of a rigorous modeling workflow, it is straightforward to determine and interpret the source of this bias through visualization of the posterior and posterior predictive distributions. It is also clear that the exact formula for the period of a simple pendulum contains the majority of relevant physics necessary to describe real data.

F. Model selection

Now that it has been established that a difference is detectable with a finite number of measurements in θ_0 , it is time to turn to the tools of Bayesian model selection to quantify when a preference for the exact expression for the period is weak, moderate, and strong. Bayesian model selection is evaluated via the Bayes factor. The Bayes factor is the ratio of Bayes evidences (the denominator of Eq. 1) between two models,

$$B_{01} = \frac{p(d|M_0)}{p(d|M_1)} \quad (6)$$

where models M_i are subscripted 0 and 1. The Bayes factor B_{01} is used to quantify model preference. Hereafter, the exact formula for the period and the small angle approximation are subscripted 0 and 1, respectively. A Bayes factor greater than one represents an increase of support for M_0 relative to M_1 and directly corresponds to the odds of $M_0:M_1$.

In addition to explicit quantification of the preference between two models, the Bayes factor allows for determination of a preferred model when the result is not immediately obvious (c.f. [6]). In the simple pendulum, a single observable – the period – is considered. However, in more sophisticated experiments, there may be multiple observables and the comparison becomes more complex. While tools such as the chi-squared per degree of freedom exist, these often make assumptions about the shape of the posterior distribution, e.g. the chi-squared test implicitly assumes normally-distributed data; the Bayes factor makes no additional distributional assumptions beyond those explicitly chosen by the priors and the likelihood. Another advantage of the Bayes factor is that it penalizes the incorporation of additional parameters. A maxim attributed to John von Neumann is that “with four parameters I can fit an elephant, and with five I can make him wiggle his trunk” [25]. It is therefore prudent to follow the guidance of William of Ockham’s Law of Parsimony: it is futile to do with more things that which can be done with fewer [26]. Accordingly, a model with many parameters should be disfavored in comparison with an equally-successful model with fewer parameters. The Bayes factor is an implementation of Occam’s Razor and requires the demand for additional complexity to come from the data itself. A further discussion of Bayesian model selection may be found in [8].

Empirical scales are used to determine when there is weak, moderate, and strong evidence for M_0 vs. M_1 . The Bayes factor is easily interpretable as it gives the direct odds ratio of one model to the other. In this work, the Jeffreys’ Scale is used (Table I), although in principle one can construct an appropriate scale for the application at hand. Data is

$ \ln B_{01} $	Odds	Probability	Strength of evidence
< 1.0	$\leq 3:1$	< 0.750	Inconclusive
1.0	$\sim 3:1$	0.750	Weak evidence
2.5	$\sim 12:1$	0.923	Moderate evidence
5.0	$\sim 150:1$	0.993	Strong evidence

TABLE I. The Jeffreys’ Scale, reproduced from [8].

generated for the model selection study as follows. Taking sufficient accurate measurements by hand is unreasonable and it has already been demonstrated that the exact expression of the period describes the motion of a pendulum well. Therefore, it is reasonable to generate data using the model, given a set of simple assumptions. It is unreasonable to assume that students would be able to make measurements at increments finer than 1° with a one-meter-long pendulum or at more than 12 increments in initial angular displacement θ_0 . Typically, students make fewer measurements in teaching laboratories and this study represents an attempt to find an idealized, maximally-restrictive constraint on initial angular displacement θ_0 .

12 proxy data points are generated if the maximum θ_0 is larger than 12° . If the maximum θ_0 is less than 12° , data is generated in 1° increments. The Bayes factor is then calculated and it is possible to interpolate between calculations with their uncertainty to determine at what $\text{Max}[\theta_0]$ the evidence for the exact model becomes weak, moderate, or strong. These data points are generated with the uncertainties commensurate with photodiode, accelerometer, and stopwatch timing as discussed in Sec. III A. Including these results demonstrates the importance of accounting for uncertainty when offering data-driven guidance and will allow for appropriate implementation of these results in the classroom.

The \ln Bayes factor is shown in Fig. 9. As anticipated, as the maximum initial angular displacement θ_0 increases, there is progressively stronger preference for the exact expression. The constraint then diminishes as the number of measurements decrease. Preference for the exact calculation at maximum initial angular displacement θ_0 is given in Table II. It

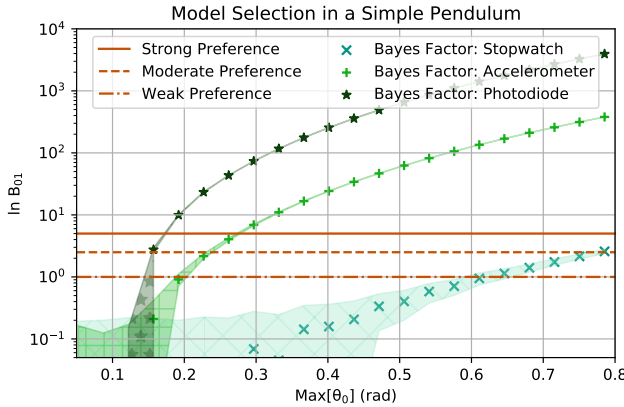


FIG. 9. (Color online) $\ln B_{01}$ demonstrating preference for the exact expression for the period of the pendulum over the small angle approximation. Positive values denote preference for the exact model. Horizontal lines denote thresholds for weak, moderate, and strong preference.

may be stated confidently that the small angle approximation is valid below these model preference thresholds.

Strength of evidence	$ \ln B_{01} $	θ_0 (rad)	θ_0 (deg)
Photodiode timing			
Weak	1.0	0.140 ± 0.003	$8.0^{+0.1}_{-0.2}$
Moderate	2.5	0.155 ± 0.002	$8.89^{+0.09}_{-0.1}$
Strong	5.0	0.171 ± 0.001	9.81 ± 0.06
Accelerometer timing			
Weak	1.0	0.195 ± 0.007	11.2 ± 0.4
Moderate	2.5	0.234 ± 0.004	$13.4^{+0.2}_{-0.3}$
Strong	5.0	0.275 ± 0.003	15.8 ± 0.2
Stopwatch timing			
Weak	1.0	$0.62^{+0.04}_{-0.03}$	35 ± 2
Moderate	2.5	0.78 ± 0.02	44.6 ± 0.9

TABLE II. Model preference thresholds in which the exact formula is preferred over the small angle approximation. Subscript 0 denotes the exact formula and subscript 1 denotes the small angle approximation. Strong preference was not found for stopwatch timing when maximum angular displacement was limited to $\pi/4$ rad.

Timing Precision	Recommended Restriction (rad)	(deg)
Photodiode ($\pm \sim 0.005$ s)	~ 0.17	~ 10
Accelerometer ($\pm \sim 0.02$ s)	~ 0.26	~ 15
Stopwatch ($\pm \sim \sqrt{2}(0.250)$ s)	$\pi/4$	45

TABLE III. Guidance for restricting initial angular displacement for simple pendula when using the small angular approximation.

V. CONCLUSIONS

This work demonstrates how to set rigorous data-driven constraints on the use of the small angle approximation in introductory physics experiments using Bayesian inference as well as how to approach statistical modeling through a workflow. This is the first instance in the literature of modern computational and statistical techniques being applied to this problem and demonstrates how the modeling procedure followed in research applications may be applied to pedagogical settings.

The heuristic guidance of constraining simple pendula to 15° is overly restrictive when timing with typical precision found in stopwatches, but is reasonable when using a smartphone accelerometer and even overly-permissive when using precise timing methods such as optical timing with photodiodes. The data does not exhibit strong preference for the exact expression with photodiode timing until 0.171 ± 0.001 radians ($9.81 \pm 0.06^\circ$) and with accelerometer timing until 0.275 ± 0.003 radians ($15.8 \pm 0.2^\circ$), while stopwatch timing is insufficiently precise to establish strong preference between the two models at maximum displacements up to $\pi/4$ radians (45°). This suggests that current guidance of restriction to $\sim 15^\circ$ is appropriate for timing of precision $\sim \pm 0.02$ s, but displacements with more precise timing ($\sim \pm 0.005$ s) should be restricted to $\sim 10^\circ$ while displacements with less precise timing commensurate with stopwatches and human reaction times should not be restricted below $\sim 45^\circ$.

This analysis represents the current state-of-the-art guidance for laboratory manuals and textbooks as it has used realistic best-case uncertainties and advanced statistical techniques to determine when the breakdown of the approximation is actually detectable. Future works should continue with the present guidance, but modify their justification to be data-driven rather than being motivated by a 1% discrepancy in the small angle approximation. This would both be more directly applicable to instructors and would more faithfully communicate to students how scientific guidance is derived. Additionally, this demonstration sets out a workflow by which students could derive their own guidance in this and other laboratory applications while gaining experience in rigorous statistical and scientific modeling.

VI. ACKNOWLEDGEMENTS

This work was supported in part by the Natural Sciences and Engineering Research Council of Canada. Thanks are due to C. Gale, N. Provatas, M. Singh, M. Frick, N. Fortier, and R. Yazdi for critical reading of the manuscript and to D. Everett for both a critical reading of the manuscript and de-

tailed discussions on the implementation of Bayesian techniques and their interpretation. R. Turner, P. Movafegh, and S. Biunno provided materials and expertise for obtaining measurements. R. Furnstahl's resources on Bayesian inference were instrumental in the development of this work. C. Gale, S. Jeon, and K. Ragan provided guidance, useful discussions, and support to this study.

- [1] F. M. S. Lima and P. Arun, “An accurate formula for the period of a simple pendulum oscillating beyond the small angle regime,” *American Journal of Physics* **74**, 892–895 (2006), <https://doi.org/10.1119/1.2215616>.
- [2] Brian S. Blais, “Model comparison in the introductory physics laboratory,” *The Physics Teacher* **58**, 209–213 (2020), <https://doi.org/10.1119/1.5145420>.
- [3] Douglas C Giancoli, *Physics: principles with applications* (Boston: Pearson, 2016).
- [4] Peter F Hinrichsen, “Review of approximate equations for the pendulum period,” *European Journal of Physics* **42**, 015005 (2020).
- [5] Rory J E Smith, Gregory Ashton, Avi Vajpeyi, and Colm Talbot, “Massively parallel Bayesian inference for transient gravitational-wave astronomy,” *Monthly Notices of the Royal Astronomical Society* **498**, 4492–4502 (2020), <https://academic.oup.com/mnras/article-pdf/498/3/4492/33798799/staa2483.pdf>.
- [6] D. Everett *et al.* (JETSCAPE), “Multi-system Bayesian constraints on the transport coefficients of QCD matter,” (2020), [arXiv:2011.01430 \[hep-ph\]](https://arxiv.org/abs/2011.01430).
- [7] Udo von Toussaint, “Bayesian inference in physics,” *Rev. Mod. Phys.* **83**, 943–999 (2011).
- [8] Roberto Trotta, “Bayes in the sky: Bayesian inference and model selection in cosmology,” *Contemporary Physics* **49**, 71–104 (2008), <https://doi.org/10.1080/00107510802066753>.
- [9] Devinderjit Sivia and John Skilling, *Data analysis: a Bayesian tutorial* (OUP Oxford, 2006).
- [10] Andrew Gelman, John B Carlin, Hal S Stern, David B Dunson, Aki Vehtari, and Donald B Rubin, *Bayesian data analysis* (CRC press, 2013).
- [11] Andrew Gelman, Aki Vehtari, Daniel Simpson, Charles C. Margossian, Bob Carpenter, Yuling Yao, Lauren Kennedy, Jonah Gabry, Paul-Christian Bürkner, and Martin Modrák, “Bayesian workflow,” (2020), [arXiv:2011.01808 \[stat.ME\]](https://arxiv.org/abs/2011.01808).
- [12] M. Betancourt, “Falling (in love with principled modeling),” (2019), betanalpha.github.io/assets/case_studies/falling.html.
- [13] Stephen D. Schery, “Design of an inexpensive pendulum for study of large-angle motion,” *American Journal of Physics* **44**, 666–670 (1976), <https://doi.org/10.1119/1.10352>.
- [14] Pauli Virtanen *et al.*, “Scipy 1.0: Fundamental algorithms for scientific computing in python,” *Nature Methods* (2020).
- [15] Private communication with instructor, “McGill University Physics 101 lab manual,” (2020).
- [16] Robert T. Wilkinson and Sue Allison, “Age and Simple Reaction Time: Decade Differences for 5,325 Subjects,” *Journal of Gerontology* **44**, P29–P35 (1989).
- [17] Stan Development team, “Prior choice recommendations,” (2020), <https://github.com/stan-dev/stan/wiki/Prior-Choice-Recommendations>.
- [18] C. Hirt and W.E. Featherstone, “A 1.5km-resolution gravity field model of the Moon,” *Earth and Planetary Science Letters* **329-330**, 22–30 (2012).
- [19] NASA, “By the numbers: Jupiter,” (2021), <https://solarsystem.nasa.gov/planets/jupiter/by-the-numbers/>.
- [20] George EP Box, “Sampling and Bayes’ inference in scientific modelling and robustness,” *Journal of the Royal Statistical Society: Series A (General)* **143**, 383–404 (1980).
- [21] Ambler Thompson and Barry N. Taylor, “Guide for the use of the international system of units (SI),” *NIST Special Publication* **811** (2008), <https://physics.nist.gov/cuu/pdf/sp811.pdf>.
- [22] W. D. Vousden, W. M. Farr, and I. Mandel, “Dynamic temperature selection for parallel tempering in Markov chain Monte Carlo simulations,” *Monthly Notices of the Royal Astronomical Society* **455**, 1919–1937 (2015), <https://academic.oup.com/mnras/article-pdf/455/2/1919/18514064/stv2422.pdf>.
- [23] <https://github.com/willvousden/ptemcee>.
- [24] Daniel Foreman-Mackey, David W. Hogg, Dustin Lang, and Jonathan Goodman, “emcee: The MCMC hammer,” *Publications of the Astronomical Society of the Pacific* **125**, 306–312 (2013).
- [25] Freeman Dyson, “A meeting with Enrico Fermi,” *Nature* **427**, 297–297 (2004).

[26] W. M. Thorburn, “The myth of Occam’s razor,” *Mind* **XXVII**, 345–353 (1918), <https://academic.oup.com/mind/article-pdf/XXVII/3/345/9877777/345.pdf>.